

Is your inflammatory disease model falling short?

See how you can model complex human immune response and drug efficacy.



WATCH NOW

The Journal of Immunology

RESEARCH ARTICLE | JANUARY 05 2024

Antiviral and Anti-Inflammatory Therapeutic Effect of RAGE-Ig Protein against Multiple SARS-CoV-2 Variants of Concern Demonstrated in K18-hACE2 Mouse and Syrian Golden Hamster Models **FREE**

Nisha Rajeswari Dhanushkodi; ... et. al

J Immunol j12300392.

<https://doi.org/10.4049/jimmunol.2300392>

Related Content

Recombinant Bacillus Calmette–Guérin Expressing SARS-CoV-2 Chimeric Protein Protects K18-hACE2 Mice against Viral Challenge

J Immunol (April,2023)

Pan-coronavirus neutralizing S2 human monoclonal antibodies and utility of direct respiratory administration as combination therapy with S1 antibodies against SARS-CoV-2

J Immunol (May,2022)

SARS-CoV-2 Spike_{395–404} is identified as a murine CD8⁺ T cell epitope in the receptor-binding domain of the SARS-CoV-2 spike protein

J Immunol (May,2022)

Antiviral and Anti-Inflammatory Therapeutic Effect of RAGE-Ig Protein against Multiple SARS-CoV-2 Variants of Concern Demonstrated in K18-hACE2 Mouse and Syrian Golden Hamster Models

Nisha Rajeswari Dhanushkodi,^{*,1} Swayam Prakash,^{*,1} Afshana Quadiri,^{*} Latifa Zayou,^{*} Ruchi Srivastava,^{*} Amin Mohammed Shaik,^{*} Berfin Suzer,^{*} Izabela Coimbra Ibraim,[†] Gary Landucci,[†] Delia F. Tifrea,[‡] Mahmoud Singer,^{*} Leila Jamal,^{*} Robert A. Edwards,[‡] Hawa Vahed,[§] Lawrence Brown,[¶] and Lbachir BenMohamed^{*,§,||,#}

SARS-CoV-2 variants of concern (VOCs) continue to evolve and reemerge with chronic inflammatory long COVID sequelae, necessitating the development of anti-inflammatory therapeutic molecules. Therapeutic effects of the receptor for advanced glycation end products (RAGE) were reported in many inflammatory diseases. However, a therapeutic effect of RAGE in COVID-19 has not been reported. In the present study, we investigated whether and how the RAGE-Ig fusion protein would have an antiviral and anti-inflammatory therapeutic effect in the COVID-19 system. The protective therapeutic effect of RAGE-Ig was determined in vivo in K18-hACE2 transgenic mice and Syrian golden hamsters infected with six VOCs of SARS-CoV-2. The underlying antiviral mechanism of RAGE-Ig was determined in vitro in SARS-CoV-2-infected human lung epithelial cells (BEAS-2B). Following treatment of K18-hACE2 mice and hamsters infected with various SARS-CoV-2 VOCs with RAGE-Ig, we demonstrated (1) significant dose-dependent protection (i.e., greater survival, less weight loss, lower virus replication in the lungs); (2) a reduction of inflammatory macrophages (F4/80⁺/Ly6C⁺) and neutrophils (CD11b⁺/Ly6G⁺) infiltrating the infected lungs; (3) a RAGE-Ig dose-dependent increase in the expression of type I IFNs (IFN- α and IFN- β) and type III IFN (IFN λ 2) and a decrease in the inflammatory cytokines (IL-6 and IL-8) in SARS-CoV-2-infected human lung epithelial cells; and (4) a dose-dependent decrease in the expression of CD64 (Fc γ R1) on monocytes and lung epithelial cells from symptomatic COVID-19 patients. Our preclinical findings revealed type I and III IFN-mediated antiviral and anti-inflammatory therapeutic effects of RAGE-Ig protein against COVID-19 caused by multiple SARS-CoV-2 VOCs. *The Journal of Immunology*, 2024, 212: 1–10.

The COVID-19 pandemic has created one of the largest global health crises in almost a century. Although the current rate of SARS-CoV-2 infections has decreased significantly, the long-term outlook of COVID-19 remains a serious cause of high death worldwide, with the mortality rate still surpassing even the worst mortality rates recorded for the influenza viruses. The continuous emergence of SARS-CoV-2 variants of concern (VOCs), including multiple heavily mutated Omicron subvariants, has prolonged the COVID-19 pandemic and outlines the urgent need for a next-generation vaccine that will protect against multiple SARS-CoV-2 VOCs. COVID-19 patients are reported with various pulmonary ailments known to be associated with the accumulation of inflammatory molecules such as advanced glycation end products (AGEs),

calprotectin, high-mobility group box family 1 (HMGB1), cytokines, angiotensin-converting enzyme 2 (ACE2), and other molecules in the alveolar space of lungs as well as in plasma (1–6). The receptor for advanced glycation end products (RAGE) is the AGE-specific multi-ligand receptor involved in inflammatory responses to various chronic inflammatory lung diseases (7, 8). RAGE is known to be highly expressed in the lungs, especially in the alveolar epithelial cells, in comparison with other organs of the human body. The RAGE pathway has been reported in the pathogenesis of lung diseases such as chronic obstructive pulmonary disease (COPD), interstitial lung diseases, and acute respiratory distress syndrome (ARDS) (9, 10). In recent years, the therapeutic intervention of the RAGE pathway has been demonstrated to benefit patients with ARDS, COPD, pulmonary

*Laboratory of Cellular and Molecular Immunology, Gavin Herbert Eye Institute, University of California, Irvine, School of Medicine, Irvine, CA; [†]High Containment Facility, University of California, Irvine, School of Medicine, Irvine, CA; [‡]Department of Pathology and Laboratory Medicine, University of California, Irvine School of Medicine, Irvine, CA; [§]Department of Vaccines and Immunotherapies, TechImmune, LLC, University Lab Partners, Irvine, CA; [¶]Galactica Pharmaceuticals, Inc., Villanova, PA; ^{||}Department of Molecular Biology & Biochemistry, University of California, Irvine, School of Medicine, Irvine, CA; and [#]Institute for Immunology, University of California, Irvine, School of Medicine, Irvine, CA

¹N.R.D. and S.P. contributed equally to this work.

ORCID: 0000-0001-8184-4050 (N.R.D.); 0000-0003-3986-890X (S.P.); 0000-0003-0212-5854 (A.Q.); 0000-0003-4563-1749 (A.M.S.); 0000-0003-4447-5385 (B.S.); 0000-0003-4649-8572 (M.S.); 0000-0001-9145-382X (R.A.E.).

Received for publication June 9, 2023. Accepted for publication November 29, 2023.

This work is supported by a grant from Galactica Pharmaceuticals, Inc.; by the Fast-Grant PR12501 from Emergent Ventures; and by U.S. Public Health Service Research

Grants A1158060, A1150091, A1143348, A1147499, A1143326, A1138764, A1124911, and A1110902 from the National Institute of Allergy and Infectious Diseases to L.B.M. and by grant R43AI174383-01 to TechImmune, LLC.

Address correspondence and reprint requests to Dr. Lbachir BenMohamed, Laboratory of Cellular and Molecular Immunology, Gavin Herbert Eye Institute, Hewitt Hall, Room 2032, 843 Health Sciences Road, Irvine, CA 92697-4390. E-mail address: lbenmoha@uci.edu

The online version of this article contains supplemental material.

Abbreviations used in this article: AAI, antiviral and anti-inflammatory; ACE2, angiotensin-converting enzyme 2; AGE, advanced glycation end product; ARDS, acute respiratory distress syndrome; ASYMP, asymptomatic; COPD, chronic obstructive pulmonary disease; mRAGE, membrane-bound receptor for advanced glycation end products; p.i., postinfection; qRT-PCR, quantitative RT-PCR; RAGE, receptor for advanced glycation end products; sRAGE, soluble receptor for advanced glycation end products; SYMP, symptomatic; VOC, variant of concern; WA, Washington strain.

Copyright © 2024 by The American Association of Immunologists, Inc. 0022-1767/24/\$37.50

fibrosis, and other pathologies associated with the pulmonary system (11–15). Notably, enhanced levels of RAGE ligands are associated with inflammatory disorder fields (16–18), such as diabetes or other chronic inflammatory disorders. This receptor has a causative effect on a range of inflammatory diseases.

In the context of COVID-19, the RAGE axis is observed to be associated with comorbidities such as COPD, coronary artery disease, atherosclerosis, and hypertension (19–29). Patients with such comorbidities are at an increased risk of exacerbation and decompensation when infected with SARS-CoV-2, given the severe inflammatory response generated. Interestingly, bronchoalveolar lavage and serum from COVID-19 patients have detectable soluble RAGE (sRAGE) protein that might potentially have a prognostic role. In COVID-19 patients, S100A12-like RAGE ligands are considered potential biomarkers that correlate with the severity of lung inflammation (2, 30). Although recent studies have explored the therapeutic interventional strategies for the RAGE pathway in chronic inflammatory diseases, strategies that modulate the RAGE pathway have yet to be studied extensively in the realm of COVID-19 (31, 32).

The RAGE receptor exists either as membrane-bound RAGE (mRAGE) or sRAGE (33). Ligands such as AGEs, S100/calgranulin, and HMGB1 protein initiate intracellular signal stimulation when linked to mRAGE (2). RAGE/AGE axis stimulation causes the downstream activation of various inflammatory transcription factors, including NF- κ B (34, 35). sRAGE can prevent ligands from binding to mRAGE, thereby inhibiting inflammatory activation (8). Isoforms of the RAGE protein, which lack the transmembrane and the signaling domain (commonly referred to as sRAGE), provide a means to develop a cure against RAGE-associated diseases.

In this study, we used a RAGE fusion protein that consists of a RAGE ligand-binding element, a heavy-chain Ig of a G4 isotype constant domain, and a linker connecting the ligand-binding element with the constant domain. This RAGE-Fc (fragment crystallizable region of the Ab) binds to ligands of RAGE through competition and inhibits RAGE signaling by competing with membrane-bound receptors for binding ligands (hereafter referred to as RAGE-Ig). We subsequently evaluated how efficiently RAGE-Ig protein may be used to treat COVID-19 in the context of multiple SARS-CoV-2 VOCs for which no effective treatment is available (2). One recent study reported the effect of RAGE antagonists to be effective against COVID-19 in the mouse model (36). To our knowledge, we are the first group to test the preclinical therapeutic effect of this RAGE-Ig fusion protein against SARS-CoV-2 VOC infection in both mouse and hamster models. Our findings also demonstrate a unique, to our knowledge, coupled antiviral and anti-inflammatory (AAI) effect of the RAGE-Ig along with the respective mechanisms involved.

Materials and Methods

Viruses

SARS-CoV-2 viruses specific to four variants, namely (1) SARS-CoV-2-USA/WA/2020 (batch number G2027B); (2) Alpha (B.1.1.7) (isolate England/204820464/2020 batch number C2108K); (3) Beta (B.1.351) (isolate South Africa/KRISP-EC-K005321/2020; batch number C2108F), and (4) Gamma (P.1) (isolate hCoV-19/Japan/TY7-503/2021; batch number G2126A) were procured from Microbiologics (St. Cloud, MN). The initial batches of viral stocks were propagated to generate high-titer virus stocks. Vero E6 (ATCC-CRL1586) cells were used for this purpose using an earlier published protocol (37). Procedures were completed only after appropriate safety training was obtained using an aseptic technique under BSL-3 containment.

Animal infection and RAGE-Ig treatment

The experiments involving usage of animal models were approved by the Institutional Animal Care and Use committee at the University of California, Irvine (Protocol number AUP-22-086). Male and female K18-hACE2 transgenic mice were intranasally infected with 1×10^4 PFU of SARS-CoV-2

(USA-WA1/2020) in 20 μ l and were treated with 100 μ g RAGE-Ig/mouse by i.p. or s.c. injection or were mock treated on alternate days ($n = 10$ each group) with 100 μ g RAGE per mouse. The RAGE-Ig treatment was administered on alternate days (beginning from day 1 to day 9 postinfection [p.i.]). Mice were monitored daily for weight loss until day 14 p.i. For the dose kinetics experiment, mice were treated with different doses of RAGE-Ig (100, 50, or 25 μ g) per mouse on alternate days (beginning from day 1 to day 9). Briefly, K18-hACE2 transgenic mice were intranasally infected with 1×10^4 PFU of SARS-CoV-2 (USA-WA1/2020) in 20 μ l and treated with RAGE-Ig (s.c.) at 100, 50, or 25 μ g/mouse/dose ($n = 4$) each on alternate days from day 1 to day 9 p.i. (1, 3, 5, 7, and 9 d p.i.) as indicated. At day 10 p.i., mice were euthanized, and immune cells from the lung were used for flow cytometry. For the hamster experiments, Syrian golden hamsters (7–8 wk old) ($n = 20$) were infected with SARS-CoV-2 Washington strain (WA) (3×10^5 PFU/hamster) or Delta (6.9×10^4 PFU/hamster). mRAGE treatment (1.5 or 3 mg/hamster) was administered by s.c. injection of RAGE-Ig or vehicle control on alternate days from day 1 to day 9 p.i., and the animals were monitored for weight loss every day until day 14 p.i.

Flow cytometry

Single-cell suspensions from the mouse lungs after collagenase treatment (10 mg/ml) for 1 h were used for FACS staining. The following Abs were used: anti-mouse CD3 (clone 17A-2, BD Biosciences), CD11c (clone HL3, BD Biosciences), CD11b (clone M1/70, BD Biosciences), F4/80 (clone BM8, BD Biosciences), F4/80, Ly6G, Ly6C, CD64, HLA-DR (clone M5/114, BD Biosciences). For surface staining, mAbs for various cell markers were added to a total of 1×10^6 cells in PBS containing 1% FBS and 0.1% sodium azide (FACS buffer) and left for 45 min at 4°C. For intracellular/intranuclear staining, cells were first treated with Cytofix/Cytoplasm (BD Biosciences) for 30 min. Upon washing with Perm/Wash buffer, mAbs were added to the cells and incubated for 45 min on ice and in the dark. Cells were washed again with Perm/TF Wash and FACS buffer and fixed in PBS containing 2% paraformaldehyde (Sigma-Aldrich, St. Louis, MO). A total of 100,000 events were acquired by the LSR II (Becton Dickinson, Mountain View, CA) followed by analysis using FlowJo software (BD Biosciences, Ashland, OR).

Histology of animal lung

Mouse lungs were preserved in 10% neutral buffered formalin for 48 h before transferring to 70% ethanol. The tissue sections were then embedded in paraffin blocks and sectioned at 8- μ m thickness. Slides were deparaffinized and rehydrated before staining for H&E for routine immunopathology.

Viral PCR assay

Lung tissue was analyzed for SARS-CoV-2-specific RNA by quantitative RT-PCR (qRT-PCR). As recommended by the Centers for Disease Control and Prevention, we used *ORF1* Ab-specific primers (forward: 5'-CCCTG TGGGTTTACACTTAA-3' and reverse: 5'-ACGATTGTGCATCAGCT GA-3') and probe (6FAM-CCGCTCTCGGATGTGGAAAGTTATGG-BHQ) to detect the viral RNA level in the lung.

PBMC isolation

Peripheral blood was collected, and PBMCs were isolated by Ficoll-Paque density gradient. The cells were washed in PBS and resuspended in a complete culture medium consisting of RPMI 1640 medium containing 10% FBS (Bio-Products, Woodland, CA) supplemented with $1 \times$ penicillin/L-glutamine/streptomycin, $1 \times$ sodium pyruvate, and $1 \times$ nonessential amino acids. About 1 million PBMCs were treated with different concentrations of RAGE-Ig, and the supernatant was used for cytokine ELISA, whereas the cells were used for flow cytometry. Human CD14⁺ monocytes were isolated from PBMCs and further differentiated into uncommitted macrophages (M0) by M-CSF. The effect of RAGE-Ig on the polarization of M0 into classically activated (M1) or activated (M2) macrophages (using a combination of IFN- γ \pm RAGE-Ig for M1 or IL-4 \pm RAGE-Ig for M2) was studied. The RAGE-Ig protein treatment causes dose-dependent morphological changes in M0 macrophages during monocyte differentiation into macrophages.

In vitro assays using a cell line

Human lung epithelial BEAS-2B cells (CRL-9609, American Type Culture Collection) were used for in vitro assays. Briefly, 1 million cells were treated with different concentrations of RAGE-Ig, and the supernatant was used for cytokine ELISA. ELISA or Luminex for various cytokines such as IFN- γ , IL-8, IL-6, IFN-B, and IFN- λ 3 was performed as per the manufacturer's (PBL Assay Science, Millipore) instructions.

Statistical analysis

Data for each assay were compared by ANOVA and Student *t* test using GraphPad Prism version 5 (GraphPad Software, La Jolla, CA). Differences between the groups were identified by ANOVA and multiple comparison procedures. Data are expressed as the mean \pm SD. Results were considered statistically significant at a *p* value ≤ 0.05 .

RAGE-Ig protein

The RAGE-Ig protein used in these studies was manufactured by Catalent Biologics (Madison, WI) and provided by Galactica Pharmaceuticals (Villanova, PA). The RAGE fusion protein comprises RAGE polypeptide sequences linked to a second, non-RAGE polypeptide. The RAGE fusion protein uses a RAGE polypeptide domain comprising a RAGE ligand binding site and an interdomain linker directly bound to an Ig C_{H2} domain. Such fusion proteins provide specific, high-affinity binding to RAGE ligands (38).

Results

Dose-dependent protection in RAGE-Ig–treated SARS-CoV-2–infected K18-hACE2 mice is associated with a decrease in lung inflammation

RAGE inhibitors may be used as novel therapeutic targets for prevention, regression, and slowing of the progression of SARS-CoV-2 infections. To examine the effect of RAGE-Ig treatment in SARS-CoV-2

infection, the best route of drug administration was studied. Mice were treated with the RAGE-Ig by either of two routes of treatment (either i.p. or s.c.) p.i. with SARS-CoV-2. Eight- to 9-wk-old male and female K18-hACE2 transgenic mice were intranasally infected with 1×10^4 PFU of SARS-CoV-2 (USA-WA1/2020) in 20 μ l treated with 100 μ g RAGE-Ig/mouse by either the i.p. (*n* = 10) or s.c. route (*n* = 10) or were mock treated (*n* = 10) on alternate days (1, 3, 5, 7, and 9 d p.i.) (Fig. 1A). Mice that were treated s.c. with 100 μ g RAGE-Ig were found to be significantly protected from weight loss and mortality (Fig. 1B). Next, we studied the dose response of RAGE-Ig fusion protein treatment on disease outcomes in SARS-CoV-2 infection. Eight- to 9-wk-old male and female K18-hACE2 transgenic mice were intranasally infected with 1×10^4 PFU of SARS-CoV-2 (USA-WA1/2020) and treated with RAGE-Ig (s.c.) at 100 μ g/mouse/dose (*n* = 4) or 50 μ g/mouse/dose (*n* = 4) or 25 μ g/mouse/dose (*n* = 4) or were mock treated (*n* = 4) on alternate days (1, 3, 5, 7, and 9 d p.i.) (Fig. 1C). We found a dose-dependent survival and weight loss benefit upon treatment with RAGE-Ig (Fig. 1D). The 100- μ g dose was found to be the most effective dose that protected against severe symptoms of COVID-19 in mice. Additionally, a significant dose-dependent decrease in inflammatory

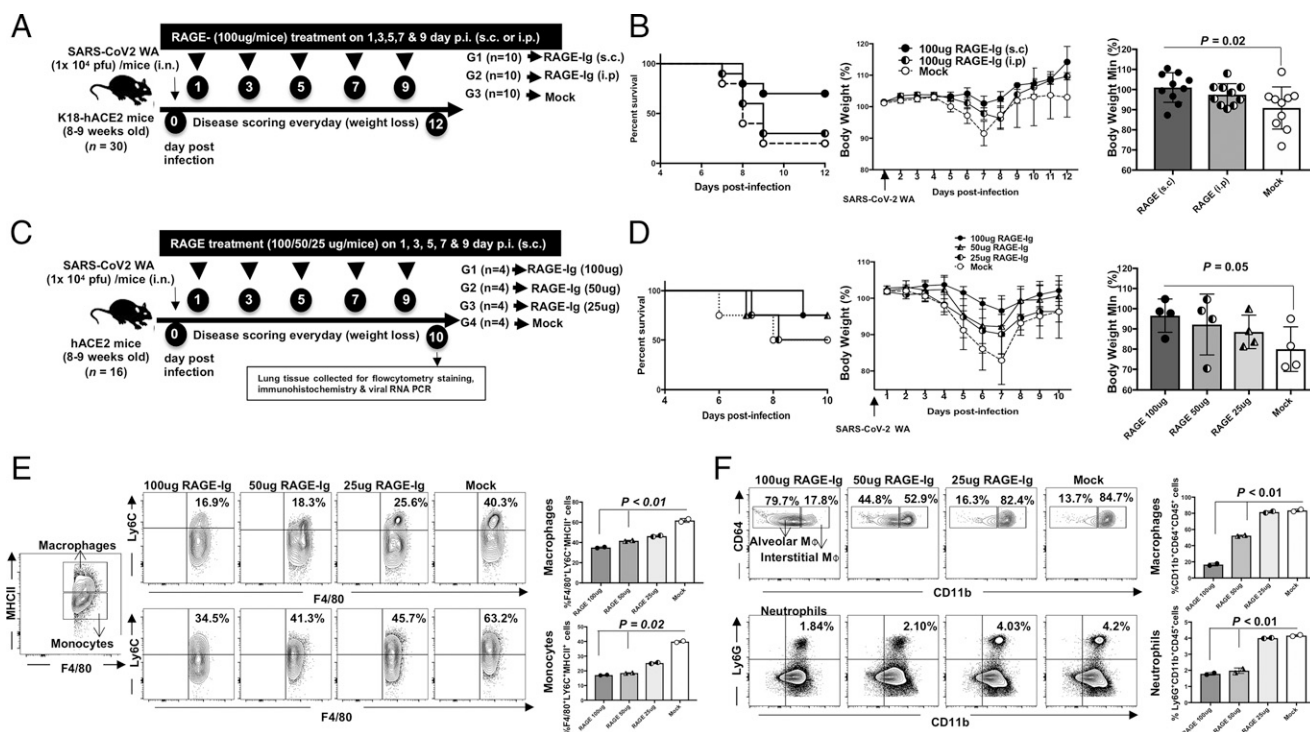


FIGURE 1. The effect of RAGE-Ig treatment on COVID-like disease and survival in ACE2 mice infected with SARS-CoV-2. **(A)** Experimental scheme to study the effect of route of administration of RAGE-Ig fusion protein on disease outcome and death in ACE2 mice infected with SARS-CoV-2 (WA strain). Mice were infected with SARS-CoV-2 (WA strain) and left untreated (Mock, *n* = 10) or were treated with RAGE-Ig s.c. (*n* = 10) or i.p. (*n* = 10). **(B)** The graph in the left panel shows the percentages of survival of ACE2 mice infected with SARS-CoV-2 and either left untreated (Mock) or treated with 100 μ g RAGE-Ig administered s.c. or i.p. The graph in the middle panel shows the average daily weight change recorded for 12 d calculated in percentages, normalized to the body weight on day 0 of infection. The bar graph in the right panel shows the maximal weight change in percentage on day 7 p.i. of ACE2 mice infected with SARS-CoV-2 and either left untreated (Mock) or treated with 100 μ g RAGE-Ig administered s.c. or i.p. **(C)** Experimental scheme to study the dose response of RAGE-Ig fusion protein treatment on survival and disease outcome in ACE2 mice infected with SARS-CoV-2. **(D)** The graph in the left panel shows the percentages of survival of ACE2 mice infected with SARS-CoV-2 and either left untreated (mock) or treated with different doses of RAGE-Ig administered s.c. The graph in the middle panel shows the average daily weight change recorded for 10 d. Bars represent the mean \pm SEM. The bar graph in the right panel shows the maximal weight change in percentage on day 7 p.i. of ACE2 mice infected with SARS-CoV-2 and either left untreated (Mock) or treated with different doses of RAGE-Ig administered s.c. **(E)** Representative (left nine panels) and average (right two panels) frequencies of F4/80⁺ LY6C⁺ MHCII⁺ macrophages (top panels) and F4/80⁺ LY6C⁺ MHCII⁺ monocytes (bottom panels) infiltrating the lungs of ACE2 mice infected with SARS-CoV-2 and either left untreated (Mock) or treated with three different doses of RAGE-Ig. **(F)** Representative (left eight panels) and average (right two panels) frequencies of macrophage subsets (top panels) and neutrophils (bottom panels) infiltrating the lungs of ACE2 mice infected with SARS-CoV-2 and either left untreated (Mock) or treated with three different doses of RAGE-Ig. The experiments were independently performed twice, and bars represent the mean \pm SEM. Data were analyzed by Student *t* test comparing RAGE-treated and untreated mice.

cells was detected in the lung interstitium of mice treated with RAGE-Ig after SARS-CoV-2 infection. Notably, high frequencies of macrophages (Ly6C⁺F4/80⁺MHCII⁺), monocytes (Ly6C⁺F4/80⁺MHCII⁻), interstitial macrophages (CD11b⁺CD64⁺CD45⁺), and neutrophils (CD11b⁺LY6G⁺CD45⁺) were detected in the lungs of RAGE-Ig-treated mice 7 d after SARS-CoV-2 infection (Supplemental Fig. 1 and Fig. 1E, 1F) (*p* value indicates the comparison between mock and 100 ng or mock and 50 ng RAGE-Ig treatment). These cells are associated with the inflammatory response in the lungs of mice infected with SARS-CoV-2. Altogether, this report suggests the potential therapeutic use of RAGE-Ig protein to attenuate macrophage-related inflammatory reactions in the treatment of COVID-19. It is noteworthy to mention that RAGE-Ig treatment not only attenuated macrophage-mediated inflammation but also reduced inflammatory neutrophil infiltration in the lungs. However, mortality and weight loss can likely be due to infection in other organs besides the lungs. This possibility will be the subject of future investigation.

RAGE-Ig treatment protects against COVID-19-like symptoms, virus replication, and mortality in K18-hACE2 mice following infection with various SARS-CoV-2 VOCs

We next determined whether RAGE-Ig treatment would be effective against the wild-type SARS-CoV-2 (USA-WA1/2020) and SARS-CoV-2 VOCs measured by disease outcome and survival in mice. Eight- to 9-wk-old male and female K18-hACE2 transgenic mice were intranasally infected with 1×10^4 PFU of SARS-CoV-2

(USA-WA1/2020) (*n* = 20), B.1.1.7 Alpha (8×10^2 PFU) (*n* = 10), B.1.351 Beta (6×10^3 PFU) (*n* = 10), and P.1 Gamma (2×10^2 PFU) (*n* = 10) variants. Subsequently, mice were treated s.c. with 100 μ g RAGE-Ig/mouse or mock treated with a buffer on alternate days (1, 3, 5, 7, and 9 d p.i.) (Fig. 2A). The inoculum for infection with wild-type SARS-CoV-2 (USA-WA1/2020) and with the various variants (B.1.1.7 Alpha, B.1.351 Beta, and P.1 Gamma) was determined on the basis of results obtained from LD₅₀ experiments done on age- and sex-matched mice and hamsters (data not shown). RAGE-Ig treatment (100 μ g) was found to significantly protect against weight loss, mortality, and viral load in USA-WA1/2020-, B.1.351 Beta-, and P.1 Gamma-infected mice (Fig. 2B). Because there was interindividual variability in weight loss for mice within each treated and untreated group, the weight loss was calculated as a percentage of initial weight for each mouse or for each group of mice. Fig. 2B also shows the individual weight loss data for each mouse within each treated and untreated group (shown as separate lines). H&E staining of lung sections demonstrated a reduction in lung pathogenicity in the RAGE-Ig-treated mice compared with mock (vehicle-treated) mice at day 14 p.i. (Fig. 2C). The most surprising result was a decrease in viral RNA in the lungs of RAGE-Ig-treated mice compared with mock-treated mice (Fig. 2B), suggesting a possible antiviral property of the RAGE-Ig compound. However, it is noteworthy to mention that the variability of lung virus titers at day 14 may reflect the variability of extrapulmonary titers and their effect on morbidity/mortality.

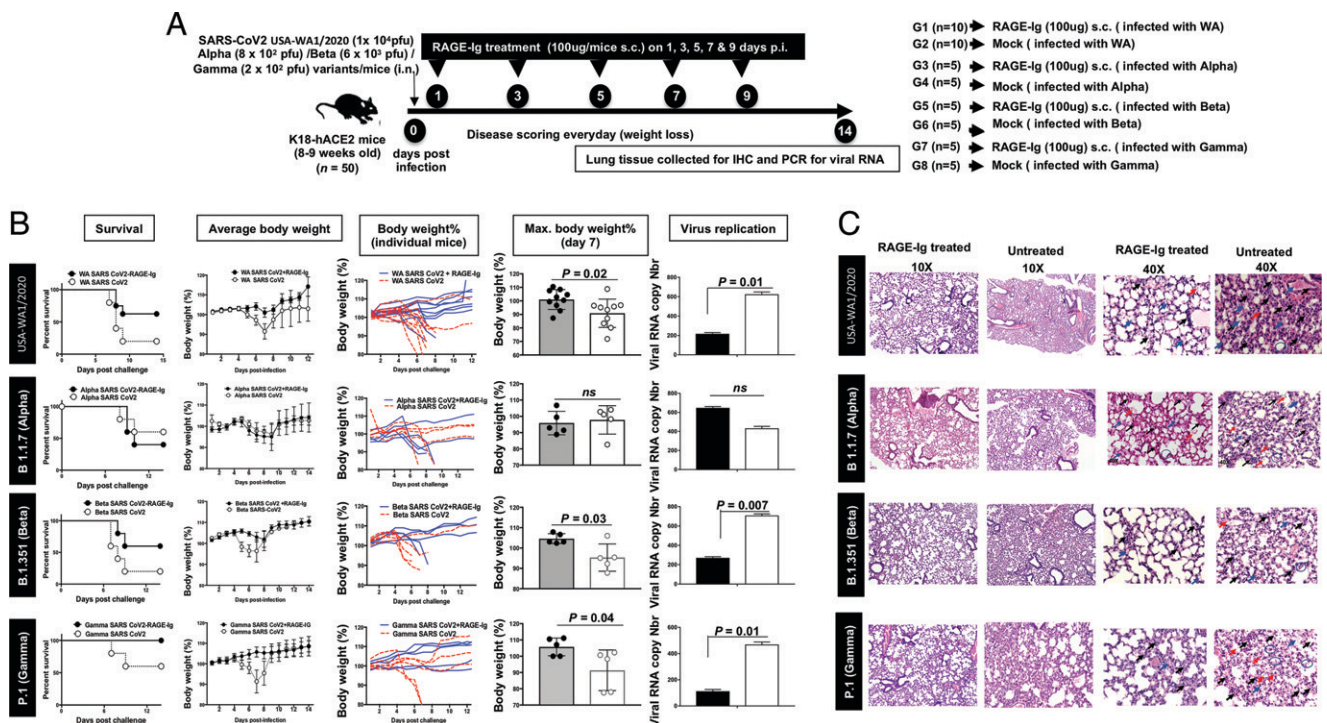


FIGURE 2. The effect of RAGE-Ig treatment on disease outcome and survival during SARS-CoV-2 VOC infection in mice. **(A)** Experimental scheme to understand the effect of RAGE-Ig treatment on survival, disease outcome, and virus replication upon infection with the SARS-CoV-2 variants. **(B)** Mice that were infected with SARS-CoV-2 and then treated with RAGE-Ig are represented as a closed black circle, and those mock infected are represented as an open white circle. The left panel shows the survival graph for each variant of SARS-CoV-2. The line graph (second to panel) shows the average weight change of 10 mice at each day p.i. normalized to the body weight on the day of infection for each VOC. The line graph (third to left panel) shows weight change for individual mice at each day p.i. normalized to the body weight on the day of infection for each variant. Bars represent the mean \pm SEM of weight change at day 7 p.i. in percentage, normalized to the body weight on the day of infection. The bar graph (right panel) shows virus replication in the lungs of RAGE-Ig-treated and untreated mice. The graph indicates fold change viral RNA copy numbers for each VOC. On day 14 p.i., mice were euthanized, and lungs were harvested and used for viral RNA quantification by qRT-PCR. **(C)** The H&E images show representative inflammatory cells infiltrating the lungs of mice infected with SARS-CoV-2 variants and treated with RAGE-Ig. At day 12 p.i., mice were euthanized, and lungs were analyzed by immunohistochemistry for pathology. The H&E images are shown at a magnification of 10 \times (left two panels) and 40 \times (right two panels). The experiments were independently performed twice, and bars represent the mean \pm SEM. Data analyzed by Student *t* tests compare RAGE-treated and untreated mice.

RAGE-Ig treatment protects Syrian golden hamsters from COVID-19 symptoms and virus replication following infection with SARS-CoV-2 WA and Delta variants

Although the protective effect of RAGE-Ig treatment against wild-type WA or VOC infection was confirmed using the mouse model, we also evaluated RAGE-Ig in the hamster model, because hamsters are outbred and recapitulate the SARS-CoV-2 pathogenicity with a higher degree of similarity to humans. Seven- to 8-wk-old male Syrian golden hamsters were intranasally infected with 1×10^5 PFU of SARS-CoV-2 (USA-WA1/2020) ($n = 10$) or B.1.617.2 Delta (6.9×10^4 PFU) ($n = 10$)/hamster in 100 μ l and followed by treatment with 1.5 mg RAGE-Ig/hamster ($n = 3$) or 3 mg RAGE-Ig/hamster ($n = 3$) by the s.c. route or mock treated with buffer ($n = 4$) on alternate days (1, 3, 5, 7, and 9 d p.i.) (Fig. 3A). Hamsters infected with SARS-CoV-2 WA or Delta virus and treated with RAGE-Ig experienced significantly less weight loss than the mock-treated group (Fig. 3B). We found reduced pathogenicity and viral load in RAGE-Ig–treated hamsters, similar to the results observed in mice. There was a decrease in viral RNA in the lungs of RAGE-Ig–treated hamsters as compared with mock-treated hamsters (Fig. 3B). Thus, our results in the hamster model confirmed the protective antiviral effect of the drug against SARS-CoV-2 infection across different models of infection.

The antiviral effect of RAGE-Ig in SARS-CoV-2–infected human lung epithelial cells is mediated by type I and type III IFNs

Our results from the mouse and hamster models revealed an antiviral effect of RAGE-Ig, which is host induced. IFNs are the major antiviral players during SARS-CoV-2 infection; hence, we studied the effect of RAGE-Ig treatment on types I, II, and III IFN secretion

in SARS-CoV-2–infected human lung epithelial cells (BEAS-2B) and its antiviral effect in infected lungs (Supplemental Fig. 2). BEAS-2B cells were infected with SARS-CoV-2 USA-WA1/2020 and treated with various concentrations of RAGE-Ig (30, 100, 250, and 500 ng/ml). Supernatants and cell lysates were collected at various time points (24, 48, and 72 h) for ELISA and qRT-PCR (Fig. 4A). There was a statistically significant decrease in viral RNA copy number at 24 h (left panel) and 48 h (right panel) in the lysates of BEAS-2B cells infected with SARS-CoV-2 following RAGE-Ig treatment as quantified by qRT-PCR (Fig. 4B), thus confirming the antiviral effect of RAGE-Ig in vitro. Simultaneously, there was an increased expression of the IFN types I and III genes at 24 h and 48 h in BEAS-2B cell lysates infected with SARS-CoV-2 following treatment with RAGE-Ig (Fig. 4C). In addition, we detected an increase in IFN- β , - γ , and - λ 3 cytokine release at 48 h p.i. in the lysates of infected BEAS-2B cells, following treatment with RAGE-Ig. From this, it may be inferred that induced antiviral IFNs, particularly types I and III, modulated SARS-CoV-2 replication in human lung epithelial cells. This could also suggest that although increased release of types I and III IFNs are associated with decreased viral replication, type II IFN- γ decreases due to the anti-inflammatory effect of RAGE-Ig protein. Thus, the modulation of the IFN pathway by RAGE-Ig protein led to a reduction in virus replication.

The anti-inflammatory effects of RAGE-Ig in SARS-CoV-2–infected human lung epithelial cells infected with SARS-CoV-2

The potential therapeutic effect of RAGE-Ig protein against SARS-CoV-2 infection in mice is partly due to a decrease in macrophage-related inflammatory cell infiltration. Although the anti-inflammatory effect of RAGE-Ig is well known, we wanted to redemonstrate this effect

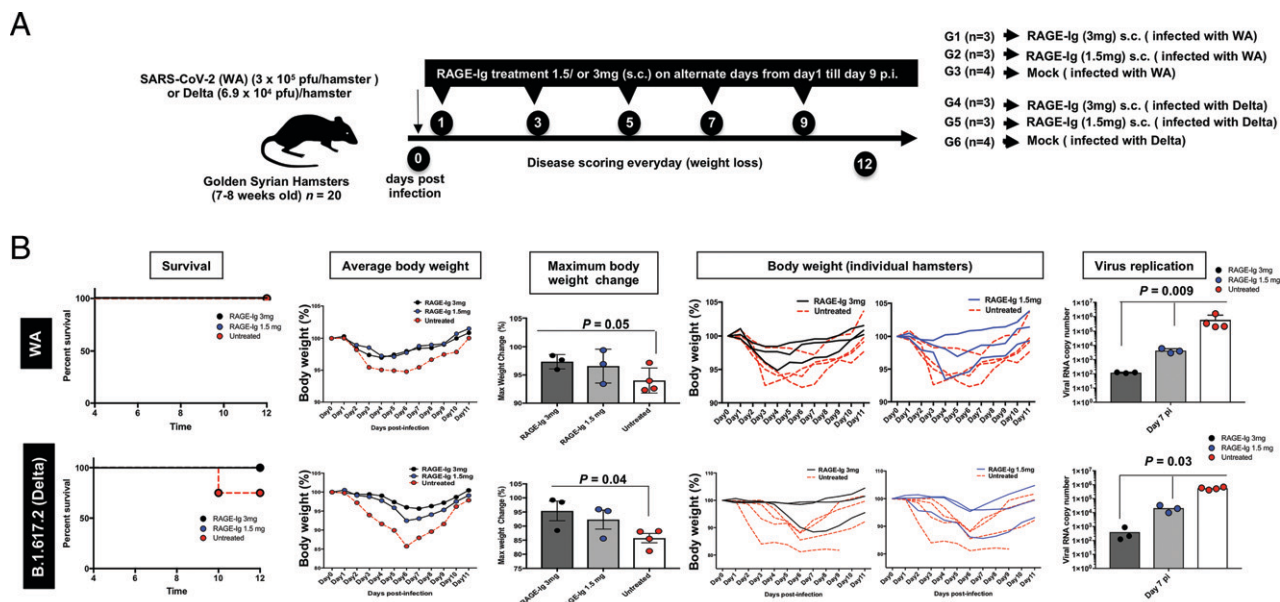


FIGURE 3. Effect of RAGE-Ig treatment on disease outcome and survival in the Syrian golden hamster infected with SARS-CoV-2 variants. **(A)** Experimental scheme to study the effect of RAGE-Ig treatment on survival, disease outcome, and virus replication in hamsters infected with SARS-CoV-2 WA or Delta variant. **(B)** Hamsters infected with SARS-CoV-2 and treated with RAGE-Ig are represented as a closed black circle (3 mg) or blue circle (1.5 mg). Mock-treated hamsters are represented as an open circle. The graph in the left panel shows the survival of treated and untreated hamsters for the WA variant (top) and Delta variant (bottom). The line graph (second to left panel) shows weight change for 14 d p.i. normalized to the body weight on the day of infection for each variant. The bar graph shows the percentage of maximum weight loss in RAGE-Ig–treated and untreated hamsters on day 8 p.i. Individual line graph (fourth and fifth panels from the left) showing weight change in individual hamsters for 11 d p.i. normalized to the body weight on the day of infection with the WA variant (top panel) and Delta variant (bottom panel). The bar graph (right panel) shows virus replication in the lungs of RAGE-Ig–treated and untreated hamsters. The graph shows a fold change in viral RNA copy numbers for each variant as indicated. At day 12 p.i., hamsters were euthanized, and lungs were used for viral RNA quantification by qRT-PCR. The experiments were independently performed twice, and bars represent the mean \pm SEM. Data analyzed by Student *t* test compare RAGE-treated and untreated hamsters.

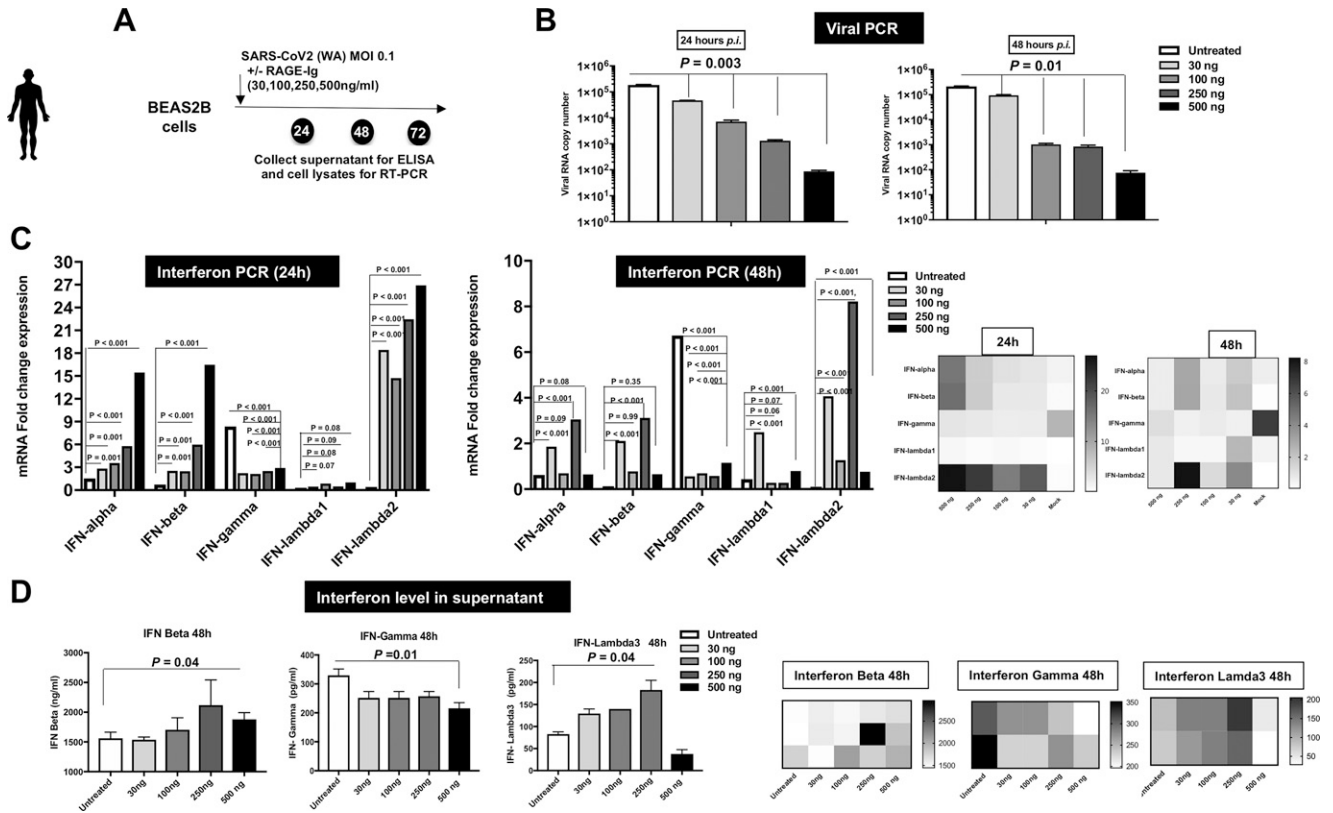


FIGURE 4. Effect of RAGE-Ig treatment on IFN types I, II, and III IFN production in vitro by SARS-CoV-2-infected human lung epithelial cells. **(A)** Experimental scheme to study the effect of RAGE-Ig treatment on production of types I, II, and III IFN in SARS-CoV-2-infected human lung epithelial cells. The BEAS-2B human lung epithelial cells are infected with SARS-CoV-2 WA and then treated with various doses of RAGE-Ig (30, 100, 250, and 500 ng/ml). Supernatant and cell lysates were collected at various time points (24, 48, and 72 h). **(B)** The graph shows viral RNA copy numbers at 24 h (left panel) and 48 h (right panel) in the lysates of BEAS-2B cells infected with SARS-CoV-2 and treated with RAGE-Ig. **(C)** The graph shows mRNA expression of IFN types I, II, and III genes at 24 h (left panel) and 48 h (middle panel) in the lysates of BEAS-2B cells infected with SARS-CoV-2 and treated with RAGE-Ig. The corresponding heat map is shown in the right panel. **(D)** Graphs show the amount of IFN- β , - γ , and - λ 3 released 48 h in the lysates of BEAS-2B cells infected with SARS-CoV-2 and treated with RAGE-Ig (left panels). The experiments were independently performed twice, and bars represent the mean \pm SEM. The p value compares the RAGE-Ig treatment at 500 ng with the mock treatment. Data analyzed by Student t test compare RAGE-treated and untreated cells.

against SARS-CoV-2 in vitro. To confirm the anti-inflammatory effect of RAGE-Ig treatment, BEAS-2B cells were infected with SARS-CoV-2 USA-WA1/2020 followed by treatment with various concentrations of RAGE-Ig (30, 100, 250, and 500 ng/ml). Supernatants were collected at multiple time points (24, 48, and 72 h) for cytokine estimation. Kinetics of the IL-6 and IL-8 cytokines released in the supernatants of BEAS-2B cells infected with SARS-CoV-2 showed a maximal release at 48 h p.i. (Fig. 5A). Additionally, we observed a significant decrease in the release of IL-6 and IL-8 cytokines at 48 h in the supernatants of BEAS-2B cells infected with SARS-CoV-2 following treatment with RAGE-Ig, which was not dose dependent (Fig. 5B). Similarly, there was a dose-dependent decrease in the levels of IL-6 and IL-8 cytokines at 48 h in the supernatants of human PBMCs infected with SARS-CoV-2 treated with RAGE-Ig (Fig. 5C). RAGE-Ig treatment ex vivo conferred anti-inflammatory effects both on the inflammatory cells from COVID-19 patients' PBMCs and on human lung epithelial cells infected with SARS-CoV-2 in vitro.

RAGE-Ig treatment affects the inflammatory profile of monocytes from COVID-19 patients

The interaction between RAGE and its ligands may ultimately activate the proinflammatory gene (39). The level of expression of RAGE ligand EN-RAGE was compared ex vivo on CD14⁺ monocytes derived from PBMCs of asymptomatic individuals (ASYMP

indicated as a black bar, $n = 5$) versus CD14⁺ monocytes derived from PBMCs of symptomatic COVID-19 patients (SYMP indicated as a gray bar, $n = 5$) (Fig. 6A). As expected, there was an increased frequency of monocytes expressing EN-RAGE ligand, suggesting increased activation of the RAGE pathway during COVID-19 pathology (40) (the error bars represent SD). To examine if RAGE-Ig treatment can modulate the expression of inflammatory receptors, PBMCs from SYMP COVID-19 patients were treated with various concentrations of RAGE-Ig (10 μ g/ml, 1 μ g/ml, 100 ng/ml, and 10 ng/ml) and analyzed by flow cytometry. RAGE-Ig treatment significantly decreased the expression of CD64 on monocytes of COVID-19 patients in a dose-dependent manner (Fig. 6B). CD64 is a high-affinity IgG receptor (Fc γ RI) that contributes to COVID-19-associated inflammation severity. Thus, RAGE-Ig treatment can potentially alleviate immune complex-mediated airway inflammation. Moreover, CD64⁺ monocytes have been implicated in antiviral immunity. To further understand whether RAGE-Ig treatment can modulate macrophage differentiation, human CD14⁺ monocytes were isolated from PBMCs and differentiated into uncommitted macrophages (M0) by M-CSF. We found that the RAGE-Ig protein treatment caused dose-dependent morphological changes in M0 macrophages during the differentiation process as shown in Fig. 6C. Flow cytometric analysis, however, did not show differential expression of known M1/M2 markers, suggesting that RAGE treatment did not affect the balance/frequency/function of M1/M2 macrophages (data not shown).

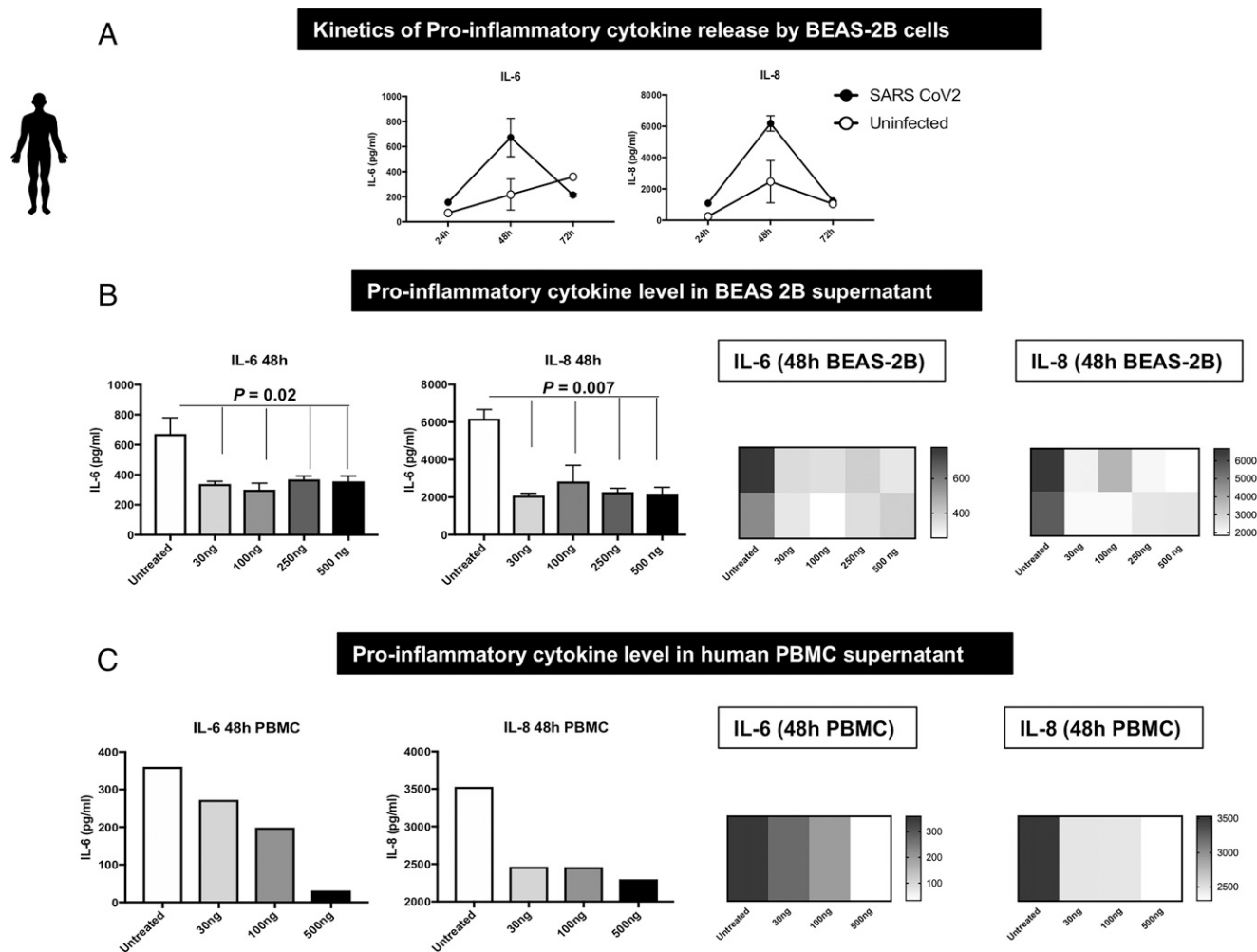


FIGURE 5. Effect of RAGE-Ig treatment on production of proinflammatory cytokines in vitro by SARS-CoV-2–infected human lung epithelial cells. BEAS-2B cells are infected with SARS-CoV-2 (WA strain) and then treated with various concentrations of RAGE-Ig (30, 100, 250, and 500 ng/ml). Supernatants were collected at various time points (24, 48, and 72 h), and the level of cytokine was determined by Luminex. **(A)** Graphs show the kinetics of IL-6 (left) and IL-8 (right) cytokines released in the supernatants of BEAS-2B cells infected with SARS-CoV-2. **(B)** Graphs show the effect of RAGE-Ig treatment on the release of IL-6 and IL-8 cytokines at 48 h in the supernatants of BEAS-2B cells infected with SARS-CoV-2 (left two panels). The corresponding heat map for cytokine release is shown in the right two panels. **(C)** Graphs show the effect of RAGE-Ig treatment on the release of IL-6 and IL-8 cytokines at 48 h in the supernatants of human PBMCs infected with SARS-CoV-2 (left two panels). The corresponding heat map for cytokine release is shown in the right two panels. The experiments were independently performed twice, and bars represent the mean ± SEM. Data analyzed by Student *t* test compare RAGE-treated and untreated cells.

Discussion

Anti-inflammatory drug interventions can be critical in preventing complications of acute COVID-19 and shortening disease recovery time in patients with long COVID. Both clinical and epidemiological evidence of COVID-19 associates age and different comorbidities with the risk of SARS-CoV-2 infection leading to severe lung involvement and disease. The association of the RAGE pathway with aging and COVID-19-associated comorbidities such as diabetes, hypertension, coronary artery disease, cardiovascular disease, renal diseases, and others suggest that intervention of the RAGE pathway may potentially be a promising therapeutic target for treating patients with preexisting conditions and severe COVID-19 symptoms (19–29). Interestingly, a recent study has reported high expression of RAGE and HMGB1 in the lung tissue of decedents with COVID-19 and diabetes. The use of RAGE inhibitors thus may be a novel therapeutic target in the prevention or slowing of the progression of SARS-CoV-2 infections that currently lack effective therapy. In this study, we explored the potential use of Galactica’s RAGE-Ig protein as a therapeutic intervention to attenuate inflammatory reactions in possible approaches for treatment against SARS-CoV-2 infection with VOCs.

For this, we first tested the drug’s therapeutic effect against the wild-type WA variant of SARS-CoV-2 infection in K18-hACE2 transgenic mice. We observed a statistically significant dose-dependent protection effect on survival and weight loss of K18-hACE2 mice infected with the WA strain of SARS-CoV-2. Importantly, we found that 100 µg of RAGE-Ig administered s.c. was the most effective dose and route of administration that protected against the symptoms of COVID-19 in mice. Subsequent experiments demonstrated that RAGE-Ig–treated mice had significantly decreased weight loss and mortality compared with mock-treated K18-hACE2 mice infected with the Beta or Gamma variant of SARS-CoV-2. For the Alpha variant, however, we could not find a benefit effect in the context of treatment with RAGE-Ig. A recent study has reported the effect of RAGE antagonist treatment in a mouse model to be effective against COVID-19 (36). To our knowledge, this is the first study to report the effect of RAGE protein on SARS-CoV-2 VOCs.

For preclinical testing, we confirmed the potential therapeutic effect of this drug at a multispecies level. We tested the drug’s effect in Syrian golden hamsters infected with WA or Delta VOCs of SARS-CoV-2. We demonstrated that the hamsters were protected

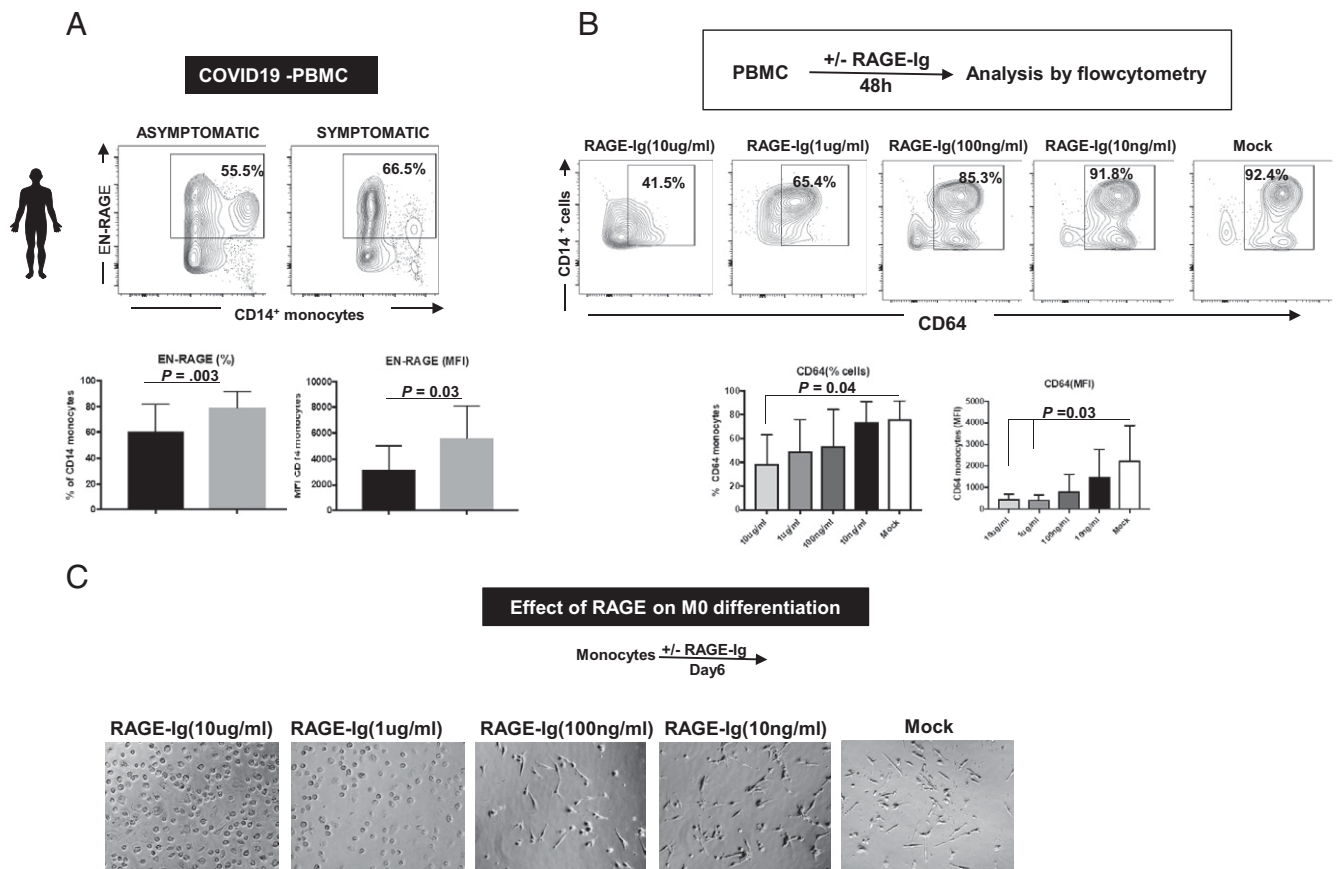


FIGURE 6. Effect of RAGE-Ig treatment on expression of inflammatory receptors on monocytes from COVID-19 patients. **(A)** The expression of RAGE ligand EN-RAGE on CD14⁺ monocytes ex vivo by PBMCs from SYMP and ASYMP COVID-19 patients detected by FACS. The representative (top panels) and average (bottom panels) data of EN-RAGE expression on CD14⁺ monocytes in ASYMP and SYMP COVID-19 patients are shown. **(B)** PBMCs from SYMP COVID-19 patients were treated with various concentrations of RAGE-Ig (10 μ g/ml, 1 μ g/ml, 100 ng/ml, 10 ng/ml), and the frequencies of CD14⁺CD64⁺ monocytes were analyzed by flow cytometry. The representative (top panels) and average (bottom panels) frequencies of CD14⁺CD64⁺ monocytes upon RAGE-Ig treatment are shown. The bottom right panel shows the effect of RAGE-Ig treatment on the level of expression of CD64 in monocytes from COVID-19 patients. **(C)** Representative microscopic images showing dose-dependent morphological changes in M0 macrophages during monocyte differentiation into a macrophage after RAGE-Ig protein treatment. Human CD14⁺ monocytes were isolated from PBMCs and further differentiated into uncommitted macrophages (M0) by M-CSF and then treated with RAGE-Ig protein (original magnification $\times 20$). The experiments were independently performed twice, and bars represent the mean \pm SEM. Data were analyzed by Student *t* test comparing RAGE-treated and untreated monocytes.

from the symptoms of SARS-CoV-2 VOC infection when treated with 1.5 or 3 mg RAGE-Ig/hamster/dose. These preclinical data demonstrated that RAGE-Ig treatment can be clinically useful in preventing complications of COVID-19 acute infection and shortening disease recovery time. Hospitalized COVID-19 patients requiring ventilation or expected to do so imminently will meet the most important clinical criteria indicating treatment with RAGE-Ig. Survival among these patients will be the primary endpoint tested in this compound's COVID-19 clinical trial.

The anti-inflammatory effect of RAGE-Ig is well established in the context of other chronic inflammatory diseases. Therefore, we intended to further understand it specifically in the context of COVID-19 infection. Due to an enhanced level of RAGE ligands in diabetes and other chronic disorders, this receptor has a causative effect in a range of inflammatory diseases. Given its inflammatory function and the ability to detect multiple ligands through a common structural motif, RAGE is often referred to as a pattern recognition receptor. EN-RAGE is a ligand for RAGE. Prior studies have demonstrated that the expression of RAGE ligand S100A12 (also known as EN-RAGE), a biomarker of pulmonary injury, increases in peripheral monocytes of COVID-19 patients. Increased EN-RAGE may promote pulmonary damage in these patients by activation of RAGE receptors on the surface of alveolar epithelial cells.

We next examined the role played by RAGE and its ligands in the disease severity of COVID-19 patients by analyzing monocytes from PBMCs of COVID-19 patients for expression of ligands and receptors of RAGE and correlation with disease severity. Instead of what was seen in previous reports, we observed an increased expression of EN-RAGE in symptomatic cases of COVID-19 compared with asymptomatic COVID-19 patients. In our study, we detected decreased expression of CD64(Fc γ R1) on monocytes upon treatment with RAGE-Ig. CD64 is a high-affinity IgG receptor (Fc γ RI) that contributes to inflammation severity in multiple disease models. Thus, RAGE-Ig treatment can potentially alleviate immune complex-mediated airway inflammation. Moreover, CD64⁻ monocytes have been implicated in antiviral immunity. Circulating monocytes differentiate upon entering tissues and are activated by cytokines or growth factors present in the lung during active infection.

Activation of uncommitted macrophages (M0) classically polarizes them into either proinflammatory M1 macrophages or anti-inflammatory M2 macrophages. Interestingly, our results showed that RAGE-Ig treatment caused a dose-dependent morphological change in M0 macrophages in vitro, thus tempting speculation that the compound can affect macrophage polarization. Upon infection, monocytes migrate into the tissues, where they become infected resident macrophages, allowing viruses to spread within tissues and organs, such as the

lungs. The SARS-CoV-2–infected lung-resident proinflammatory M1 macrophage produces large amounts of proinflammatory cytokines and chemokines, known as the cytokine storm, leading to an excessive, uncontrolled local tissue inflammatory response with tissue damage. All this could result in acute respiratory illness, known as SARS, characterized by fever, productive cough, shortness of breath/dyspnea, and pneumonia-like symptoms. Both local tissue inflammation and the cytokine storm play an immunopathological role in developing COVID-19–related complications, such as ARDS, the main cause of death in COVID-19 patients. A molecular treatment that would reduce the development of proinflammatory M1 macrophages or directly inhibit the production of proinflammatory cytokines and chemokines is urgently needed to reduce ARDS. Interestingly, we also observed a dose-dependent decreased infiltration of neutrophils (CD11b/Ly6G) and inflammatory macrophages (F4/80/Ly6C) following treatment with RAGE-Ig in SARS-CoV-2–infected mouse lung samples. In addition, we also found decreased interstitial/exudative macrophages in SARS-CoV-2–infected mouse lungs treated with RAGE-Ig.

The current protocols for the treatment of COVID-19 are based largely on the use of anti-inflammatory compounds such as dexamethasone, baricitinib, and/or mAbs, molnupiravir and nirmatrelvir/ritonavir, among others. There is a critical need for other medicinal agents, especially those with dual AAI activity, that would be readily available for the early treatment of mild to moderate COVID-19 in high-risk patients. Interestingly, we noticed that RAGE-Ig treatment not only protected from symptoms of SARS-CoV-2 infection but also decreased the viral titers of SARS-CoV-2 in the lungs of treated animals. This will greatly improve the survival outcomes of ventilated COVID-19 patients by shortening their ICU stays and reducing their viral load. Although the underlying causes of long COVID-19, which may affect at least 10% of all those infected with COVID-19, are not yet well understood, clinicians believe that long COVID symptoms are caused by residual inflammation and/or viral load. If this hypothesis is correct, the RAGE-Ig protein may also be an effective therapy for long COVID with its unique dual AAI activity. Our results showed variable levels of protection in RAGE-Ig–treated mice following infection with different SARS-CoV-2 variants. The difference in levels of protection may be due to variations in the virulence of each variant and the severity of pathologies induced in mice by each variant.

Due to its rare dual properties of AAI activity, the RAGE-Ig protein, with its broad preclinical efficacy, is a promising drug candidate for COVID-19 treatment. To confirm whether the RAGE-Ig treatment induced any antiviral effect, we conducted a series of in vitro studies of the drug using a human lung epithelial cell line (BEAS-2B). We demonstrated the role of the IFN pathway in the antiviral mechanisms induced during RAGE-Ig treatment of lung epithelial cells. RAGE-Ig treatment of SARS-CoV-2–infected epithelial cells caused a dose-dependent decrease in viral RNA copy number, which in turn was found to correspond to an increase in type I and type III IFNs, as demonstrated by both qRT-PCR and ELISA. Our findings suggest that RAGE-Ig treatment increased types I and III IFN but not type II IFN (IFN- γ) response in human lung epithelial cells infected with SARS-CoV-2.

It is established that type I IFN signaling leads to antiviral ISG expression (via IRF3 and IRF7), whereas type II IFN signaling leads to proinflammatory gene expression (via NF- κ B signaling). An unbalanced immune response, characterized by a weak production of type I IFNs (IFN-Is) and an exacerbated release of proinflammatory cytokines, contributes to the severe forms of the disease. Thus, RAGE-Ig treatment during SARS-CoV-2 infection may suppress inflammatory cytokine responses (such as IL-6 and IL-8) and enhance types I and III IFN (IFN- β and IFN- λ) responses, resulting in less severe disease.

Our results indicate a dual AAI activity and significant therapeutic potential for Galactica's RAGE-Ig protein against COVID-19 caused by emerging VOCs. The therapeutic effect of RAGE-Ig on SARS-CoV-2 infection is mediated through an anti-inflammatory and host-directed antiviral effect by type I and type III IFNs.

Acknowledgments

We thank UC Irvine's Medical Center and Institute for Clinical and Translational Science for helping with blood drawing from COVID-19 symptomatic and asymptomatic individuals for this study.

Disclosures

The authors have no financial conflicts of interest.

References

- Lim, A., A. Radujkovic, M. A. Weigand, and U. Merle. 2021. Soluble receptor for advanced glycation end products (sRAGE) as a biomarker of COVID-19 disease severity and indicator of the need for mechanical ventilation, ARDS and mortality. *Ann. Intensive Care* 11: 50.
- Yalcin Kehribar, D., M. Cihangiroglu, E. Sehmen, B. Avcı, A. Capraz, A. Yildirim Bilgin, C. Gunaydin, and M. Ozgen. 2021. The receptor for advanced glycation end product (RAGE) pathway in COVID-19. *Biomarkers* 26: 114–118.
- Chiappalupi, S., L. Salvadori, A. Vukasinovic, R. Donato, G. Sorci, and F. Ruzzi. 2021. Targeting RAGE to prevent SARS-CoV-2-mediated multiple organ failure: hypotheses and perspectives. *Life Sci.* 272: 119251.
- Jabaudon, M., P. Berthelin, T. Pranal, L. Roszyk, T. Godet, J. S. Faure, R. Chabanne, N. Eisenmann, A. Lautrette, C. Belville, et al. 2018. Receptor for advanced glycation end-products and ARDS prediction: a multicentre observational study. *Sci. Rep.* 8: 2603.
- Kerkeni, M., and J. Gharbi. 2020. RAGE receptor: may be a potential inflammatory mediator for SARS-CoV-2 infection? *Med. Hypotheses* 144: 109950.
- Salehi, M., S. Amiri, D. Ilghari, L. F. A. Hasham, and H. Piri. 2022. The remarkable roles of the receptor for advanced glycation end products (RAGE) and its soluble isoforms in COVID-19: the importance of RAGE pathway in the lung injuries. *Indian J. Clin. Biochem.* 38: 159–171.
- Bierhaus, A., P. M. Humpert, M. Morcos, T. Wendt, T. Chavakis, B. Arnold, D. M. Stern, and P. P. Nawroth. 2005. Understanding RAGE, the receptor for advanced glycation end products. *J. Mol. Med. (Berl.)* 83: 876–886.
- Oczyppok, E. A., T. N. Perkins, and T. D. Oury. 2017. All the “RAGE” in lung disease: the receptor for advanced glycation endproducts (RAGE) is a major mediator of pulmonary inflammatory responses. *Paediatr. Respir. Rev.* 23: 40–49.
- Calfee, C. S., L. B. Ware, M. D. Eisner, P. E. Parsons, B. T. Thompson, N. Wickham, M. A. Matthay, and N. A. Network; NHLBI ARDS Network. 2008. Plasma receptor for advanced glycation end products and clinical outcomes in acute lung injury. *Thorax* 63: 1083–1089.
- Nakamura, T., E. Sato, N. Fujiwara, Y. Kawagoe, S. Maeda, and S. Yamagishi. 2011. Increased levels of soluble receptor for advanced glycation end products (sRAGE) and high mobility group box 1 (HMGB1) are associated with death in patients with acute respiratory distress syndrome. *Clin. Biochem.* 44: 601–604.
- Jabaudon, M., R. Blondonnet, L. Roszyk, D. Bouvier, J. Audard, G. Clairefond, M. Fournier, G. Marceau, P. Déchelotte, B. Pereira, et al. 2015. Soluble receptor for advanced glycation end-products predicts impaired alveolar fluid clearance in acute respiratory distress syndrome. *Am. J. Respir. Crit. Care Med.* 192: 191–199.
- Blondonnet, R., J. Audard, C. Belville, G. Clairefond, J. Lutz, D. Bouvier, L. Roszyk, C. Gross, M. Lavergne, M. Fournet, et al. 2017. RAGE inhibition reduces acute lung injury in mice. *Sci. Rep.* 7: 7208.
- Sim, Y. S., D. G. Kim, and T. R. Shin. 2016. The diagnostic utility and tendency of the soluble receptor for advanced glycation end products (sRAGE) in exudative pleural effusion. *J. Thorac. Dis.* 8: 1731–1737.
- Sharma, A., S. Kaur, M. Sarkar, B. C. Sarin, and H. Changotra. 2021. The AGE-RAGE axis and RAGE genetics in chronic obstructive pulmonary disease. *Clin. Rev. Allergy Immunol.* 60: 244–258.
- Machahua, C., A. Montes-Worboys, L. Planas-Cerezales, R. Buendia-Flores, M. Molina-Molina, and V. Vicens-Zygmunt. 2018. Serum AGE/RAGES as potential biomarker in idiopathic pulmonary fibrosis. *Respir. Res.* 19: 215.
- Tian, J., A. M. Avalos, S. Y. Mao, B. Chen, K. Senthil, H. Wu, P. Parroche, S. Drabic, D. Golenbock, C. Sirois, et al. 2007. Toll-like receptor 9-dependent activation by DNA-containing immune complexes is mediated by HMGB1 and RAGE. [Published erratum appears in 2007 *Nat. Immunol.* 8: 780.] *Nat. Immunol.* 8: 487–496.
- Hofmann, M. A., S. Drury, B. I. Hudson, M. R. Gleason, W. Qu, Y. Lu, E. Lalla, S. Chitnis, J. Monteiro, M. H. Stickland, et al. 2002. RAGE and arthritis: the G82S polymorphism amplifies the inflammatory response. *Genes Immun.* 3: 123–135.
- Ekong, U., S. Zeng, H. Dun, N. Feirt, J. Guo, N. Ippagunta, J. V. Guarrera, Y. Lu, A. Weinberg, W. Qu, et al. 2006. Blockade of the receptor for advanced glycation end products attenuates acetaminophen-induced hepatotoxicity in mice. *J. Gastroenterol. Hepatol.* 21: 682–688.
- Kuba, K., Y. Imai, and J. M. Penninger. 2006. Angiotensin-converting enzyme 2 in lung diseases. *Curr. Opin. Pharmacol.* 6: 271–276.

20. Forbes, J. M., S. R. Thorpe, V. Thallas-Bonke, J. Pete, M. C. Thomas, E. R. Deemer, S. Bassal, A. El-Osta, D. M. Long, S. Panagiotopoulos, et al. 2005. Modulation of soluble receptor for advanced glycation end products by angiotensin-converting enzyme-1 inhibition in diabetic nephropathy. *J. Am. Soc. Nephrol.* 16: 2363–2372.
21. Dozio, E., C. Sitzia, L. Pistelli, R. Cardani, R. Rigolini, M. Ranucci, and M. M. Corsi Romanelli. 2020. Soluble receptor for advanced glycation end products and its forms in COVID-19 patients with and without diabetes mellitus: a pilot study on their role as disease biomarkers. *J. Clin. Med.* 9: 3785.
22. De Francesco, E. M., V. Vella, and A. Belfiore. 2020. COVID-19 and diabetes: the importance of controlling RAGE. *Front. Endocrinol. (Lausanne)* 11: 526.
23. Rojas, A., I. Gonzalez, and M. A. Morales. 2020. SARS-CoV-2-mediated inflammatory response in lungs: should we look at RAGE? *Inflamm. Res.* 69: 641–643.
24. Stilhano, R. S., A. J. Costa, M. S. Nishino, S. Shams, C. S. Bartolomeo, A. C. Breithaupt-Faloppa, E. A. Silva, A. L. Ramirez, C. M. Prado, and R. P. Ureshino. 2020. SARS-CoV-2 and the possible connection to ERs, ACE2, and RAGE: focus on susceptibility factors. *FASEB J.* 34: 14103–14119.
25. Loomis, S. J., Y. Chen, D. B. Sacks, E. S. Christenson, R. H. Christenson, C. M. Rebholz, and E. Selvin. 2017. Cross-sectional analysis of AGE-CML, sRAGE, and esRAGE with diabetes and cardiometabolic risk factors in a community-based cohort. *Clin. Chem.* 63: 980–989.
26. Gutierrez-Mariscal, F. M., M. P. Cardelo, S. de la Cruz, J. F. Alcalá-Díaz, I. Roncero-Ramos, I. Guler, C. Vals-Delgado, A. López-Moreno, R. M. Luque, J. Delgado-Lista, et al. 2021. Reduction in circulating advanced glycation end products by mediterranean diet is associated with increased likelihood of type 2 diabetes remission in patients with coronary heart disease: from the Cordioprev Study. *Mol. Nutr. Food Res.* 65: 1901290.
27. Šebeková, K., Z. Krivošíková, and M. Gajdoš. 2014. Total plasma Nε-(carboxymethyl)-lysine and sRAGE levels are inversely associated with a number of metabolic syndrome risk factors in non-diabetic young-to-middle-aged medication-free subjects. *Clin. Chem. Lab. Med.* 52: 139–149.
28. Farhangi, M. A., P. Dehghan, and N. Namazi. 2020. Prebiotic supplementation modulates advanced glycation end-products (AGEs), soluble receptor for AGEs (sRAGE), and cardiometabolic risk factors through improving metabolic endotoxemia: a randomized-controlled clinical trial. *Eur. J. Nutr.* 59: 3009–3021.
29. Koyama, H., S. Tanaka, M. Monden, T. Shoji, T. Morioka, S. Fukumoto, K. Mori, M. Emoto, T. Shoji, M. Fukui, et al. 2014. Comparison of effects of pioglitazone and glimepiride on plasma soluble RAGE and RAGE expression in peripheral mononuclear cells in type 2 diabetes: randomized controlled trial (PiORAGE). *Atherosclerosis* 234: 329–334.
30. Wong, L. S. Y., E. X. L. Loo, A. Y. H. Kang, H. X. Lau, P. A. Tambyah, and E. H. Tham. 2020. Age-related differences in immunological responses to SARS-CoV-2. *J. Allergy Clin. Immunol. Pract.* 8: 3251–3258.
31. Kim, H. J., M. S. Jeong, and S. B. Jang. 2021. Molecular characteristics of RAGE and advances in small-molecule inhibitors. *Int. J. Mol. Sci.* 22: 6904.
32. Bierhaus, A., and P. P. Nawroth. 2009. Multiple levels of regulation determine the role of the receptor for AGE (RAGE) as common soil in inflammation, immune responses and diabetes mellitus and its complications. *Diabetologia* 52: 2251–2263.
33. Neeper, M., A. M. Schmidt, J. Brett, S. D. Yan, F. Wang, Y. C. Pan, K. Elliston, D. Stern, and A. Shaw. 1992. Cloning and expression of a cell surface receptor for advanced glycosylation end products of proteins. *J. Biol. Chem.* 267: 14998–15004.
34. Huttunen, H. J., C. Fages, and H. Rauvala. 1999. Receptor for advanced glycation end products (RAGE)-mediated neurite outgrowth and activation of NF-kappaB require the cytoplasmic domain of the receptor but different downstream signaling pathways. *J. Biol. Chem.* 274: 19919–19924.
35. Yeh, C. H., L. Sturgis, J. Haidacher, X. N. Zhang, S. J. Sherwood, R. J. Bjercke, O. Juhasz, M. T. Crow, R. G. Tilton, and L. Denner. 2001. Requirement for p38 and p44/p42 mitogen-activated protein kinases in RAGE-mediated nuclear factor-kappaB transcriptional activation and cytokine secretion. *Diabetes* 50: 1495–1504.
36. Jessop, F., B. Schwarz, D. Scott, L. M. Roberts, E. Bohrsen, J. R. Hoidal, and C. M. Bosio. 2022. Impairing RAGE signaling promotes survival and limits disease pathogenesis following SARS-CoV-2 infection in mice. *JCI Insight* 7: e155896.
37. Case, J. B., A. L. Bailey, A. S. Kim, R. E. Chen, and M. S. Diamond. 2020. Growth, detection, quantification, and inactivation of SARS-CoV-2. *Virology* 548: 39–48.
38. Koch, M., S. Chitayat, B. M. Dattilo, A. Schiefner, J. Diez, W. J. Chazin, and G. Fritz. 2010. Structural basis for ligand recognition and activation of RAGE. *Structure* 18: 1342–1352.
39. Chuah, Y. K., R. Basir, H. Talib, T. H. Tie, and N. Nordin. 2013. Receptor for advanced glycation end products and its involvement in inflammatory diseases. *Int. J. Inflamm.* 2013: 403460.
40. Curran, C. S., and J. B. Kopp. 2022. RAGE pathway activation and function in chronic kidney disease and COVID-19. *Front. Med. (Lausanne)* 9: 970423.